Associations between human bacterial pathogens and ARGs are magnified in leachates as landfill ages

Dong Wu[1,2], Liuhong Wang[1], Yinglong Su[1,2], Jan Dolfing[3], Bing Xie[1,2*]

[1] Key Laboratory for Urban Ecological Processes and Eco-Restoration, School of Ecological and Environmental Science, East China Normal University, Shanghai 200241, China

[2] Shanghai Institute of Pollution Control and Ecological Security, Shanghai 200092, China

[3] Faculty Energy and Environment, Northumbria University, Newcastle upon Tyne NE1 8QH, UK

*Corresponding author: Prof. Bing Xie
East China Normal University
Shanghai 200062
P.R. China
Email: bxie@des.ecnu.edu.cn
Phone: (+86) 021-54341276

*Highlights (3 to 5 bullet points (maximum 85 characters including spaces per bullet point)

Highlights

- Target ARGs became increasingly associated with pathogens in leachates
- Integrons were not directly related to the enhanced “pathongen-ARGs” associations
- Bacteria with higher N-metabolizing capacity outcompeted other phyla in leachates
- Pathogens are more likely to acquire ARGs in a less diverse bacterial community

Graphic Abstract

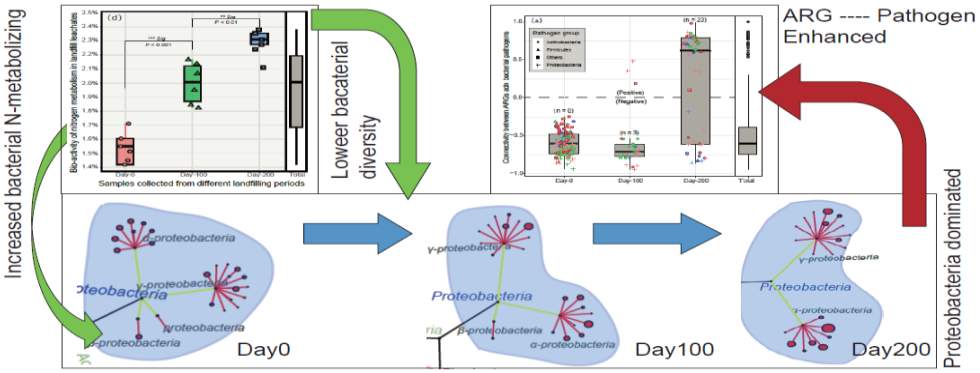

Abstract

Landfills constitute the largest treatment and disposal reservoirs of anthropogenic waste on earth and they are continuously releasing antibiotic resistance genes (ARGs) to the environment for decades via leachates. Little is known about the association between ARGs and human bacterial pathogens as a function of time. Here, we quantified 10 subtypes of ARGs, integrons, and human bacterial pathogens (HBPs). Except for the ARGs encoding resistance to sulfonamides, the subtypes encoding resistance to beta-lactams, macrolides, and aminoglycosides were not related to integrons (Spearman, $P > 0.05$). Over time presence of ARGs became increasingly more correlated with the presence of human bacterial pathogens (Procrustes test; $R = 0.81$, $P < 0.05$), which were primarily identified as the *Proteobacteria*, *Actinobacteria*, and *Firmicutes*. Rather than the prevalence of integrons, dynamics of the bacterial community, including the increased nitrogen metabolism activity of *Proteobacteria* and decreased bacterial diversity were assumed to lead to a magnified association between HBPs and target ARGs (Varpart; > 13%).

Keywords: Antibiotic resistance; Human bacterial pathogens; Landfills; Nitrogen metabolism capacity; Solid waste treatment.

1. Introduction

Sir Alexander Fleming may have hardly anticipated that his serendipitous discovery of penicillin used to control bacterial diseases, which heavily caused human mortality in the pre-antibiotic era (Tomasz, 2006), is now leading human beings to another "Dark Age" by the middle of the 21st century due to the misuse and overuse of antibiotics (de Kraker et al., 2016). The antibiotic resistome not only adapts to the clinical antibiotics (Stoesser et al., 2016) but also expands to natural environments (Shen et al., 2018). The efficient exchange of antibiotic resistance genes (ARGs) between environmental bacteria and human pathogens highlights the riks of the ARGs out of clinical settings (Vikesland et al., 2017). In effect, the rampant dissemination of antibiotic resistance (AR) from soil (Fang et al., 2015), water/wastewater (Hendriksen et al., 2019), and air (Xie et al., 2019) to human beings has triggered increased concerns from scientific communities and administrative authorities worldwide (Sugden et al., 2016). The currently proposed AR-combating frameworks have prioritized the surveillance of ARGs' mobilization to human pathogens (WHO, 2014), strict management of antibiotic-containing waste (Larson, 2015), and construction of a "one-health" system (Robinson et al., 2016).

Landfills, as the largest anthropogenic waste treatment and disposal sites on our planet (Wilson et al., 2015), have been included in a holistic AR monitoring and management system (Pruden et al., 2013). Although recent studies have confirmed the MSW as AR

sources in landfills (Sun et al., 2016), none of them focused on the relationships between human bacterial pathogens (HBPs) and ARGs, which can be readily released into the neighboring environments for more than 20 years via leachates (Wu et al., 2017). Antibiotic-resistant HBPs, such as *Klebsiella pneumonia*, are commonly detected in the treated wastewater (Prado et al., 2008). Some commensal HBPs like fecal coliforms are also found to carry clinically important emerging ARGs (Walsh et al., 2011; Shen et al., 2018). However, the bacterial AR in anthropogenic waste and wastewater as not required to be routinely monitored. Thus, to analyze how HBPs are related to the AR during the landfilling process becomes a critical environmental health question awaiting a thorough answer.

From the perspective of bacteria (Wu et al., 2018a), the spread of ARGs in the microbial community is influenced by surrounding nutrients and antimicrobial (response to stresses) levels. This is usually considered as a microbial evolutionary strategy to reduce the fitness (*e.g.* growth rates) of mutated bacterial strains for their survival in presence of antibiotics (Reznick and King, 2017). However, there seemed no need for bacteria to counter antibiotics, which were detected lower than the sub-inhibitory concentrations in landfills (Reznick and King, 2017). Significant correlations between the ARGs and antibiotics have indeed not been commonly observed (Wu et al., 2015a; Sun et al., 2016; Yu et al., 2016). However, ARGs can propagate through the community and this process can be affected by the environmental factor in aqueous environments

(Zhu et al., 2017). In landfills, nitrogen is the most dynamic environmental element: N is gradually metabolized by microbes from organic-N, to ammonium-N, and finally to nitrogen gas (Kjeldsen et al., 2002), resulting in decreasing nitrogen contents (500-5000 mg/L) and the changed structure of the bacterial community in leachates (Wu et al., 2015b). N-induced variations in microbial communities are known to affect the distribution of ARGs within these communities (Forsberg et al., 2014). But till now, the relationships between ARGs, bacterial community compositions, with special attention for the presence of human pathogens, have never been evaluated.

Here, we collected leachates from an MSW landfill column over more than 300 days and analyzed for the presence of ARGs and HBPs, the structure of the bacterial community, and the microbial functions involved in nitrogen metabolism. The objectives of this study were to i) evaluate the occurrences of and associations between ARGs and HBPs, and ii) analyze the impacts of the whole bacterial community dynamics on shaping the associations between ARGs and HBPs.

2. Materials and Methods

2.1 Description of landfill operation and sampling.

Leachates were sampled from six landfill columns (1.5m in height×0.2m in diameter) in parallel, all of which were filled with 65 kg of MSW disposed of in Shanghai Lao-gang MSW Treatment Center. This MSW treatment center harbors the largest landfill

system in Asia and processes 10,000 - 15,000 tons of MWS per day. The average composition of MSW in the landfill column was provided in Supplementary Information (SI-1; **Fig. S1**). The column was covered with a water-sealed lid to maintain an anaerobic condition and was operated continuously for one year. The experiment was separated into different stages based on the operational periods, which included three stages: first 60 days since commencement (Stage-1), the following 100 days (Stage-2), and 200 days (Stage-3). Leachate samples were collected in triplicates from the bottom of the MSW landfill column every 10-15 days (**Fig. S1**), which were immediately placed in sealed cool boxes after sampling.

2.2 Pretreatment of leachates and DNA extraction

Sampled leachates (50 mL) were centrifuged at 10000 x g for 10 min. The concentrate was filtered through a sterile 0.45 μm PES membrane filters (MembraneSolutions Allpure, Shanghai). The pellets were lyophilized and preserved together with membrane filters at -40℃ for subsequent DNA extraction. PowerSoil DNA Isolation Kit (MOBIO, USA) was used for DNA extraction according to the manufacturer's protocol. The yield and quality of the DNA extractions were verified by spectrophotometry ($1.8 < OD_{260/280} < 2.0$; Merinton 4000, China). The DNA extracts from membranes and pellets, which stemmed from the same one sample, were combined and were stored at - 20 °C for further analysis.

2.3 Real-Time quantitative polymerase chain reaction (qPCR)

All DNA samples were diluted by 10-20%, to concentrations between 1 and 5 ng/μL, to reduce the related interferences to amplification reactions. The target genes included class A (*bla*$_{TEM}$) and D β-lactamase genes (*bla*$_{OXA}$), which are resistant to the 3rd - Gen β-lactams (blaR). Other target ARGs included *aad*A1 and *str*B, which are resistant to aminoglycosides (AgyR); *tet*M and *tet*Q, which are resistant to TCs (tetR); *sul1*and *sul2*, which are resistant to sulfonamides (sulR); *erm*B and *mef*A, which are resistant to MLs (MLsR). In addition, two MGEs markers (inl1 and intl2) were detected, which represented the abundance of class 1 and 2 integrons, respectively.

The quantification of all target genes was performed on a BioRad CFX96 Touch system (BioRad, USA) in triplicates. All qPCR reactions were run simultaneously with seven times serially diluted standards of known quantities ($\times10^{-2}$ to $\times10^{-8}$). Information regarding the quality control, qPCR protocols, reaction systems, and information on primers were provided in Supplementary Information (**Table S1**; SI-2).

2.4 Measurement of physicochemical factors

The COD values of each sample were measured via Vario TOC Select (Elementar GmbH, Germany); the ammonia (NH_4+-N), nitrate and nitrite (NOx-N), total nitrogen (TN), and total phosphorus (TP) concentrations were detected by using an automated discrete analyzer (SmartChem-200, Italy). Handheld instruments were used to detect

115 the pH (PH-Scan, Shanghai) and DO (HI9147, Hanna, Italy) contents of leachates on
116 the outlets of the landfill columns (**Fig. S1**).

117 *2.5 Illumina HiSeq amplicon-sequencing of 16S rRNA gene*

118 To assess the diversity and relative abundances of bacteria in all samples, the V1 – V3
119 region of the bacterial 16S rRNA gene was barcoded, amplified and sequenced on an
120 Illumina Hiseq2500 platform (PersonalBio, Shanghai). The sequencing data were
121 analyzed by using Mothur protocol (Version 1.35) (Schloss et al., 2009). The paired-
122 end sequencing reads with sequence lengths less than 150 bp and-or with more than
123 two ambiguous nucleotides were removed. There were around 120,000 clean
124 sequencing reads of each sample utilized for the subsequent analysis. The quality-
125 filtered reads were further trimmed for the chimera check by using VSEARCH (Rognes
126 et al., 2016). The resulting high-quality sequences (425 – 475 bp) were assembled into
127 operational taxonomic units (OTUs) at a 97% identity threshold. Taxonomy was
128 assigned using the most updated high-quality ribosomal RNA databases (SILVA
129 Release 132) (Quast et al., 2013). The paired Illumina sequencing data are available at
130 Sequence Read Archive (PRJNA543733) with the accession number of SRP198965.

131 *2.6 BLASTn of bacterial pathogens*

132 Sequences were identified as originating from pathogens based on the comprehensive
133 list of 155 HBP species in the China CDC database (Miao et al., 2017). All filtered

high-quality 16S rRNA gene sequences from each sample were merged and assembled by using BBMap (Bushnell et al., 2017). All the merged contigs were selected from each sample and then were locally aligned against (blast-n) the constructed database with an E-value < 1×10^{-10}. After that, only the best-match alignment results were collected and the results having a matching length no less than 350 b were filtered to annotate the bacterial pathogen species by the strict identity of N>=99% (Chen et al., 2016). The relative abundances of identified HBPs were calculated according to **Eq. 1**, where the $N._{aligned\_count}$ represented the number of alignment hits of each HBPs taxa.

$$\text{HBPs (\%)} = 100\% \times \frac{N.aligned\_count}{\sum_1^n aligned\ reads\ counts} \qquad (\textbf{Eq.1})$$

2.7 Prediction of functions of bacterial community

All sequence reads were processed by the pipeline of the SILVA rRNA gene database project (SILVAngs 1.3) (Quast et al., 2013). The uploaded reads matching less than 50 aligned nucleotides or having more than 2% of ambiguities were removed. The resulting identical reads were identified and the unique reads were clustered as OTUs (similarity = 97%; overhangs <= 1) in each sample (Li and Godzik, 2006), which was further processed by a local nucleotide BLAST search (Camacho et al., 2009), against the non-redundant version of the SILVA SSU Ref dataset (release 132). The OTUs assigned to taxonomic information was output as the SILVAngs fingerprints. The obtained taxonomic profiles were initially linked to a set of pre-computed metabolic

reference profiles through the fast method Taxy-Pro (Klingenberg et al., 2013) and the predicted metabolic reference profiles (based on the KEGG database) was conducted through the SILVAngs webserver (Asshauer et al., 2015).

2.8 Data analysis.

Excel 2010 (Microsoft, USA) was used to conduct descriptive statistics (e.g. calculation of average values, standard deviation, and outliners). The mean and standard deviation values were kept to one decimal place. For samples collected in the same operational stage, their data were grouped for analyses. The statistical analysis was performed in Canoco version 5.0 software and R3.5.3. The significance was defined by 95% confidence intervals ($P < 0.05$, two-tail) unless stated otherwise. Spearman method were used to analyze the correlations between bacteria and ARGs (**Table S2**). Details of statistical methods are provided in Supplementary Information (SI-3).

3. Results

3.1 Relative abundances of target ARGs in leachates.

There were 10 subtypes of ARGs quantified using qPCR in all leachate samples. As shown in **Fig. 1**, the summed contents of blaR genes were widely ranged from 0 to -5.5 $\log_{10}$(copies/16S rRNA gene)) and exhibited a stepwise decrease with the progression of landfilling (Kruskal-Wallis test (KW); $\chi^2 = 4.6$, $P = 0.05$). Among the blaR genes,

171 *bla*$_{TEM}$ and *bla*$_{OXA}$ were detected as major ARG subtypes in the Stage-1 (-2.2 ± 1.5
172 $\log_{10}$(copies/16S rRNA gene)) and Stage-3 (-1.4 ± 0.6 $\log_{10}$(copies/16S rRNA gene)),
173 respectively (**Fig. 1**). The relative abundances of AgyR and MLsR genes were kept at
174 a stable level of ~ 2.2 $\log_{10}$(copies/16S rRNA gene) during the whole landfilling period
175 (One-way ANOVA, $P > 0.05$). Notably, *strB* (- 1.3 ± 0.4 log10(copies/16S rRNA gene)),
176 and *ermB* (- 2.5 ± 0.5 log10(copies/16S rRNA gene)) were observed as the dominant
177 subtypes with respect to conferring the AgyR and MLsR resistances.

178 Genes encoding sulR were the most abundant ARGs (1.1 ± 0.5 $\log_{10}$(copies/16S rRNA
179 gene)), particularly of *sul1*, which was 2 orders of magnitudes higher than *sul2* and
180 significantly increased from 0.5 to 1.5 $\log_{10}$(copies/16S rRNA gene) as landfill aged
181 (One-way ANOVA, F=66.7, $P < 0.001$). By contrast, the mean abundance of target tetR
182 genes exhibited a substantial decline from -2.5 to -3.5 $\log_{10}$(copies/16S rRNA gene))
183 during the experimental period (KW test; $\chi^2 = 12.3$, $P = 0.002$; **Fig. 1**). This was mainly
184 contributed by the decrease of *tetM*, which was the dominant component of tetR genes.

185 *3.2 Variations of integrons and contents of physicochemical factors*.

186 During the landfilling process (**Table 1**), the relative abundances of the integron marker
187 genes (*intl1* and *intl2*) varied significantly (KW test, $\chi^2 = 13.0$, $P = 0.001$). As the major
188 subtype, *intl1* was enriched by 0.5 orders of magnitude from Stage-1 to Stage-3 (-1.3
189 $\log_{10}$(copies/16S rRNA gene)), whereas the relative abundance of *intl2* was firstly

decreased from -2.7 to -3.6 $\log_{10}$(copies/16S rRNA gene) and then increased to -2.8 $\log_{10}$(copies/16S rRNA gene) in leachates of Stage-3 (**Table 1**). Leachates sampled in the present study were generally neutral (pH 7.3-7.7; **Table 1**). Their DO values, except for Stage-2 samples (0.9 ± 0.6 mg/L), were all above 1.0 mg/L. Interestingly, higher DO values of Stage-1 samples were detected with higher nitrate/nitrite contents (10 – 20 mg/L; **Table 1**). Apart from that, the contents of TN (3500 – 600 mg/L), NH_4^+-N (700 – 170 mg/L), and TP (6 -0.5 mg/L) all held a declining tendency along with the landfilling process (One-way ANOVA, $P < 0.05$). The concentration of COD increased to 572.3 ± 141.0 mg/L in Stage-2 leachates and then decreased to 392.6 ± 154.2 in Stage-3 ones (One-way ANOVA, F=6.3, $P < 0.001$; **Table 1**).

3.3 Dynamics of bacterial community from Stage-1 to Stage-3.

The bacterial community in landfill leachates appeared to become less diverse, which was reflected by a continuous decrease of the Shannon Index from Stage-1 to Stage-3 (6.7 to 5.9; **Table S3**). Meanwhile, the bacterial compositions at the phylum level were also observed with distinct differences from Stage-1 to Stage-3 (**Fig. 2**; ANOSIM, R = 0.67, $P < 0.01$). **Fig. 2** shows that the bacterial profiles, based on the Bray-Curtis distance, in the Stage-1 leachates were more closely inner-related than that of any other samples. *Proteobacteria*, *Bacteroidetes*, *Firmicutes*, and *Actinobacteria* accounted for 45% ~ 65% of the total bacterial abundance across all samples. *Proteobacteria* accounted for the largest portion of the bacterial community of all leachate samples

(17.9 ± 8.2%) and their abundance significantly increased from 11.5 ± 3.7% at Stage-1 to 28.1 ± 10.1% at Stage-3 (Paired T-test; $P = 0.03$). This increase was primarily caused by the variations of α- and γ-*Proteobacteria* (**Fig. 2**). *Bacteroidetes* being the second largest bacterial phylum (10.7 ± 5.0%), decreased by half during the landfilling process (Wilcoxon test; $P < 0.01$), whose dominant class was *Bacteroidia* (**Fig. 2**). Similarly, the relative abundance of *Firmicutes* experienced a drastic decline from the Stage-1 to Stage-2 (14.0 ± 1.2 vs. 1.9 ± 0.6%; KW test, $P = 0.38$), during which the *Clostridia* was detected as the dominant subtaxon class and its abundance was the highest in the Stage-1 samples (> 2.5%; **Fig. 2**). *Actinobacteria*, whose relative abundance kept at ~ 3.0% in all leachate samples (KW test, $P = 0.24$), was majorly represented by the classes of *Actinobacteria* (0.4 ± 0.2%) and *Coriobacteriia* (0.6 ± 0.7%) at the class level.

3.4 Abundance and distribution of HBPs in landfill leachates

The identified HBPs in leachate belonged to the phyla of *Proteobacteria*, *Firmicutes*, and *Actinobacteria* (**Fig. 3**). Variations in HBPs' abundances were mainly observed on the phyla of *Firmicutes* and *Proteobacteria* (**Fig. 3**). During the landfilling process (**Fig. S2**), the total relative abundance of *Firmicutes*-HBPs decreased significantly from 0.07% to 0.01% (KW test, $\chi^2 = 4.1$, $P = 0.05$), especially for the *Enterococcus faecium* and *Clostridium difficile* (**Fig. S3**). A similar trend was also observed on *Actinobacteria* pathogens (from 0.17% to 0.07%; **Fig. S2**), which includes species like *Dermatophilus congolensis* and *Mycobacterium spp*. (**Fig. S3**). Notably, *Actinobacteria* and

Proteobacteria dominated the distribution profile of total bacterial pathogens in both of Stage-2 and Stage-3 samples (**Fig. 3**), whereas the identified HBPs belonging to some high AR risk *Proteobacteria*, such as *Pseudomonas aeruginosa*, *Legionella pneumophila*, and *Legionella bozemanae* (WHO 2017), had the highest abundance (~ 0.3%; **Fig. S3**) and they slightly increased from Stage-1 to Stage-3.

4. Discussion

Landfill leachate has been recognized as an important gateway of AR from MSW to the natural environments (Graham et al., 2011; Wu et al., 2018b). The ARGs that are hosted by HBPs are considered to have the highest AR risk (Martinez et al., 2015). Within a global context of the ever-increasing landfilling rates and AR hazards (Powell et al., 2015; Cassini et al., 2019), it is critically important to understand how the variations of different types of ARGs are related to HBPs in leachates, which we reported for the first time.

Generally, the relationships between ARGs and bacterial pathogens changed over time (**Fig. 4**). It was not until the Stage-3 (**Fig. 4a**), that target ARGs became positively related to the HBPs (number of positive correlation = 23), especially to those belonging to the phylum of *Proteobacteria* (**Fig. 4a**). For example, *Acinetobacter baumannii*, *Klebsiella pneumonia*, *Pseudomonas aeruginosa*, and *Legionella pneumophila* were strongly correlated with tetracycline-resistant genes in Stage-3 (Spearman; $R > 0.70$, *P*

< 0.05; **Table S2**). This is consistent with the observations on the HBPs (**Fig. 3**), the distribution of which was majorly influenced by the *Proteobacteria* HBPs, while the *Proteobacteria* predominated the whole bacteria community during the whole experiments (**Fig. 2**). Notably, although the abundance of *Firmicute* HBPs decreased as the landfill aged, significant correlations of *Bacillus anthracis* with blaR genes were only detected at Stage-3 (**Fig.4a**; Spearman; R = 0.81, $P < 0.01$). Regarding the *Actinobacteria*, their subtaxon HBPs including *Mycobacterium cheloei* and *Nocardia farcinica* were significantly related to MLsR and tetR genes in Stage-3 (**Fig.4a**).

As shown in **Fig. 4b**, structural associations between the HBPs and ARGs fluctuated substantially across different landfilling periods (Procrustes; $P = 0.04$, $M^2 = 0.43$). However, not all ARGs were closely structured with HBPs as the landfill was aging. For example, there were no HBPs possessing linkages with either *sul1* or *sul2* (**Table S2**). This may suggest that the prevalence of integrons was only related to the increase of target sulR genes (Pearson, $P = 0.001$; **Fig. 1**), which may alienate the relationships between ARGs and their bacterial hosts. The increased connectivity between pathogens and target ARGs could result from the dynamics of the whole bacterial community (Pehrsson et al., 2016). As shown in **Fig. 5**, the major HBPs were classified as α- and γ-*Proteobacteria*, which was analogous to the phylogenic classification of the total *Proteobacteria* (**Fig. 2**); and the HBPs belonging to *Actinobacteria* and *Firmicutes*, their relative abundances also fluctuated by a similar pattern to that of their parent phyla.

The variation-based matrix correlation analyses further proved the HBPs to be closely associated with bacterial community (Mantel test; permutations = 999, R = 0.51, P = 0.03).

As an energy pathway, nitrogen metabolism can alter the composition of the bacterial community, thereby influencing the distribution of the resistome in the environment (Forsberg et al., 2014; Wu et al., 2019). Nitrogen metabolism functional genes were recently observed to widely co-exist with ARGs in the bacterial community and the *Proteobacteria* were detected as the predominant bacterial hosts (Wang et al., 2020). In leachate samples, the variations of predicted N-functional genes (**Table S3**) were significantly associated with the distribution of total bacteria at the phylum level (Mantel test; permutations = 999, R = 0.60, P = 0.001). Furthermore, the relative abundance of *Proteobacteria*, being the primary bacterial phylum (**Fig. 2**), fitted a positive linear regression with the bioactivity of nitrogen metabolism (Pearson; R = 0.70, $P < 0.01$; **Fig. 6**). The high nitrogen metabolism capacity of *Proteobacteria* have been well-documented (Delmont et al., 2018), the growth of which was favored in the nitrogen-rich environments (Dai et al., 2018). This significant correlation, together with the aforementioned co-development of the "pathogen - whole bacterial" community (**Fig. 5**), suggests the relevance of *Proteobacteria* as the predominant bacteria linking its subtaxon pathogens and N-metabolizing activity in leachates. Although HBPs community profiles and nitrogen metabolism pathways were not significantly related

(Mantel test; $P = 0.14$), the distribution of HBPs was still pronouncedly affected by the bio-activity of nitrogen metabolism in leachates (Varpart, > 13%; **Table S4**). Meanwhile, *Proteobacteria* as the most influential bacteria explained ~ 8% of the variations (**Table S4**). This might imply that by acquiring increasingly more energy from nitrogen metabolism, *Proteobacteria* gradually dominated the bacterial community (**Fig. 2**), which simultaneously facilitated the reproduction of *Proteobacteria* HBPs (**Fig. 5**).

In addition, the predominance of *Proteobacteria* over the whole bacterial community led to a relatively low bacterial diversity in the leachates at Stage-3 (**Table S3**). As reported by Mahnert et al. (2019), the loss of microbial diversity and the transition from Gram-positive *Actinobacteria*-dominated to Gram-negative *Proteobacteria*-dominated bacterial community (**Fig. 2** and **Fig. 3**) coincided with an increase in antibiotic resistance. Acquisition of ARGs reduced the growth and reproduction rates of antibiotic-resistant bacteria (Reznick and King, 2017), which made them less fitted to their living environments than other bacteria, but a less diverse bacterial community lowered the fitness costs on ARG-hosting bacteria (Vaz-Moreira et al., 2014). Therefore, it is plausible that the HBPs identified at Stage-3 (lowest Shannon index = 5.9; **Table S3**) were prone to become ARG carriers (**Fig. 4b**); and the fitness cost could become less to the predominant *Proteobacteria*, which were predicted to have nitrogen-metabolism advantages in the nitrogen-rich leachates (**Fig. 6**).

5. Conclusions

Release of ARGs from landfills is a long-term process, during which the associations between ARGs and HBPs were magnified as the landfill was aging. However, this phenomenon is not simple. In our case, *Proteobacteria* outcompeted other phyla in abundance due to their strong nitrogen metabolizing capacity. Meantime, the observed shifts in the bacterial community were co-occurred with the enrichment of *Proteobacteria* HBPs and reduction on bacterial diversity, both of which were assumed to be ideal conditions for the dissemination of ARGs among the HBPs. Hence, more efficient management of MSW to separate out the nitrogen-rich organic waste, such as via composting, before landfill is necessary in terms of the control of ARGs.

Acknowledgments

This work is supported by the Natural Science Foundation of China (21577038, 31370510) and Shanghai Tongji Gao-Tingyao Environ. Sci. Technol. Development Foundation (STGEF2017). The authors thank Mgr. H. Huang (LG Wastes Disposal Co. LTD) and Dr. Liu Hang for their supports in on-site landfill sampling and bioinformatics (Hong Kong Polytechnic University), respectively. Dong Wu would specifically like to thank The Society of Hong Kong Scholar for its supports in his postdoctoral research (XJ2018030).

The authors declare no conflict of interest.

Supplementary Information

The supplementary Information (SI) is comprised of three sections: SI-1) physicochemical composition of landfill samples; SI-2) molecular tests information and SI-3) additional statistics. The paired Illumina sequencing data are available at Sequence Read Archive (PRJNA543733) with the accession number of SRP198965 (status: published).

References

Asshauer, K.P., Wemheuer, B., Daniel, R., Meinicke, P., 2015. Tax4Fun: predicting functional profiles from metagenomic 16S rRNA data. Bioinformatics 31, 2882-2884.

Bushnell, B., Rood, J., Singer, E., 2017. BBMerge - Accurate paired shotgun read merging via overlap. PloS one 12, e0185056.

Camacho, C., Coulouris, G., Avagyan, V., Ma, N., Papadopoulos, J., Bealer, K., Madden, T.L., 2009. BLAST+: architecture and applications. BMC Bioinformatics 10, 421.

Cassini, A., Högberg, L.D., Plachouras, D., Quattrocchi, A., Hoxha, A., Simonsen, G.S., Colomb-Cotinat, M., Kretzschmar, M.E., Devleesschauwer, B., Cecchini, M., Ouakrim, D.A., Oliveira, T.C., Struelens, M.J., Suetens, C., Monnet, D.L., Strauss, R., Mertens, K., Struyf, T., Catry, B., Latour, K., Ivanov, I.N., Dobreva, E.G., Tambic Andraševic, A., Soprek, S., Budimir, A., Paphitou, N., Žemlicková, H., Schytte Olsen, S., Wolff Sönksen, U., Märtin, P., Ivanova, M., Lyytikäinen, O., Jalava, J., Coignard, B., Eckmanns, T., Abu Sin, M., Haller, S., Daikos, G.L., Gikas, A., Tsiodras, S., Kontopidou, F., Tóth, Á., Hajdu, Á., Guólaugsson, Ó., Kristinsson, K.G., Murchan, S., Burns, K., Pezzotti, P., Gagliotti, C., Dumpis, U., Liuimiene, A., Perrin, M., Borg, M.A., de Greeff, S.C., Monen, J.C.M., Koek, M.B.G., Elstrøm, P., Zabicka, D., Deptula, A., Hryniewicz, W., Caniça, M., Nogueira, P.J., Fernandes, P.A., Manageiro, V., Popescu, G.A., Serban, R.I., Schréterová, E., Litvová, S., Štefkovicová, M., Kolman, J., Klavs, I., Korošec, A., Aracil, B., Asensio, A., Pérez-Vázquez, M., Billström, H., Larsson, S., Reilly, J.S., Johnson, A., Hopkins, S., 2019. Attributable deaths and disability-adjusted life-years caused by infections with antibiotic-resistant bacteria in the EU and the European Economic Area in 2015: a population-level modelling analysis. The Lancet. Infect. Dis. 19, 56-66.

Chen, B., Yuan, K., Chen, X., Yang, Y., Zhang, T., Wang, Y., Luan, T., Zou, S., Li, X., 2016. Metagenomic Analysis Revealing Antibiotic Resistance Genes (ARGs) and Their Genetic Compartments in the Tibetan Environment. Environ. Sci. Technol. 50, 6670-6679.

Dai, Z., Su, W., Chen, H., Barberan, A., Zhao, H., Yu, M., Yu, L., Brookes, P.C., Schadt, C.W., Chang, S.X., Xu, J., 2018. Long-term nitrogen fertilization decreases bacterial diversity and favors the growth of Actinobacteria and Proteobacteria in agro-ecosystems across the globe. Glob. Chang. Biol. 24, 3452-3461.

de Kraker, M.E.A., Stewardson, A.J., Harbarth, S., 2016. Will 10 Million People Die a Year due to Antimicrobial Resistance by 2050? Plos Med. 13.

Delmont, T.O., Quince, C., Shaiber, A., Esen, O.C., Lee, S.T., Rappe, M.S., McLellan, S.L., Lucker, S., Eren, A.M., 2018. Nitrogen-fixing populations of Planctomycetes and Proteobacteria are abundant in surface ocean metagenomes. Nat. Microbiol. 3, 804-813.

Fang, H., Wang, H., Cai, L., Yu, Y., 2015. Prevalence of antibiotic resistance genes and bacterial pathogens in long-term manured greenhouse soils as revealed by metagenomic survey. Environ. Sci. Technol. 49, 1095-1104.

Forsberg, K.J., Patel, S., Gibson, M.K., Lauber, C.L., Knight, R., Fierer, N., Dantas, G., 2014. Bacterial phylogeny structures soil resistomes across habitats. Nature 509, 612-616.

Graham, D.W., Olivares-Rieumont, S., Knapp, C.W., Lima, L., Werner, D., Bowen, E., 2011. Antibiotic resistance gene abundances associated with waste discharges to the Almendares River near Havana, Cuba. Environ. Sci. Technol. 45, 418-424.

Hendriksen, R.S., Munk, P., Njage, P., van Bunnik, B., McNally, L., Lukjancenko, O., Roder, T., Nieuwenhuijse, D., Pedersen, S.K., Kjeldgaard, J., Kaas, R.S., Clausen, P., Vogt, J.K., Leekitcharoenphon, P., van de Schans, M.G.M., Zuidema, T., de Roda Husman, A.M., Rasmussen, S., Petersen, B., Amid, C., Cochrane, G., Sicheritz-Ponten, T., Schmitt, H., Alvarez, J.R.M., Aidara-Kane, A., Pamp, S.J., Lund, O., Hald, T., Woolhouse, M., Koopmans, M.P., Vigre, H., Petersen, T.N., Aarestrup, F.M., 2019. Global monitoring of antimicrobial resistance based on metagenomics analyses of urban sewage. Nature Commun. 10, 1124.

Kjeldsen, P., Barlaz, M.A., Rooker, A.P., Baun, A., Ledin, A., Christensen, T.H., 2002. Present and Long-Term Composition of MSW Landfill Leachate: A Review. Crit. Rev. Environ. Sci. Technol. 32, 297-336.

Klingenberg, H., Assauer, K.P., Lingner, T., Meinicke, P., 2013. Protein signature-based estimation of metagenomic abundances including all domains of life and viruses. Bioinformatics 29, 973-980.

Larson, C., 2015. China's lakes of pig manure spawn antibiotic resistance. Science 347, 704.

Li, W., Godzik, A., 2006. Cd-hit: a fast program for clustering and comparing large sets of protein or nucleotide sequences. Bioinformatics 22, 1658-1659.

Mahnert, A., Moissl-Eichinger, C., Zojer, M., Bogumil, D., Mizrahi, I., Rattei, T., Martinez, J.L., Berg, G., 2019. Man-made microbial resistances in built environments. Nature Commun. 10, 968.

Martinez, J.L., Coque, T.M., Baquero, F., 2015. What is a resistance gene? Ranking risk in resistomes. Nat. Rev. Microbiol. 13, 116-123.

Miao, J., Han, N., Qiang, Y., Zhang, T., Li, X., Zhang, W., 2017. 16SPIP: a comprehensive analysis pipeline for rapid pathogen detection in clinical samples based on 16S metagenomic sequencing. BMC Bioinformatics 18, 568.

Pehrsson, E.C., Tsukayama, P., Patel, S., Mejia-Bautista, M., Sosa-Soto, G., Navarrete, K.M., Calderon, M., Cabrera, L., Hoyos-Arango, W., Bertoli, M.T., Berg, D.E., Gilman, R.H., Dantas, G., 2016. Interconnected microbiomes and resistomes in low-income human habitats. Nature 533, 212-216.

Powell, J.T., Townsend, T.G., Zimmerman, J.B., 2015. Estimates of solid waste disposal rates and reduction targets for landfill gas emissions. Nat. Clim. Change 6.

Prado, T., Pereira, W.C., Silva, D.M., Seki, L.M., Carvalho, A.P., Asensi, M.D., 2008. Detection of extended-spectrum beta-lactamase-producing Klebsiella pneumoniae in effluents and sludge of a hospital sewage treatment plant. Lett. Appl. Microbiol. 46, 136-141.

Pruden, A., Larsson, D.G., Amezquita, A., Collignon, P., Brandt, K.K., Graham, D.W., Lazorchak, J.M., Suzuki, S., Silley, P., Snape, J.R., Topp, E., Zhang, T., Zhu, Y.G., 2013. Management options for reducing the release of antibiotics and antibiotic resistance genes to the environment. Environ. Sci. Persp. 121, 878-885.

Quast, C., Pruesse, E., Yilmaz, P., Gerken, J., Schweer, T., Yarza, P., Peplies, J., Glockner, F.O., 2013. The SILVA ribosomal RNA gene database project: improved data processing and web-based tools. Nucleic. Acids Res. 41, D590-596.

Reznick, D., King, K., 2017. Antibiotic resistance: Evolution without trade-offs. Nat. Ecol. Evol. 1, 0066.

Robinson, T.P., Bu, D.P., Carrique-Mas, J., Fevre, E.M., Gilbert, M., Grace, D., Hay, S.I., Jiwakanon, J., Kakkar, M., Kariuki, S., Laxminarayan, R., Lubroth, J., Magnusson, U., Thi Ngoc, P., Van Boeckel, T.P., Woolhouse, M.E., 2016. Antibiotic resistance is the quintessential One Health issue. Transactions of the Royal Society of Tropical Medicine and Hygiene 110, 377-380.

Rognes, T., Flouri, T., Nichols, B., Quince, C., Mahe, F., 2016. VSEARCH: a versatile open source tool for metagenomics. PeerJ. 4, e2584.

Schloss, P.D., Westcott, S.L., Ryabin, T., Hall, J.R., Hartmann, M., Hollister, E.B.,

Lesniewski, R.A., Oakley, B.B., Parks, D.H., Robinson, C.J., Sahl, J.W., Stres, B., Thallinger, G.G., Van Horn, D.J., Weber, C.F., 2009. Introducing mothur: open-source, platform-independent, community-supported software for describing and comparing microbial communities. Appl. Environ. Microbiol. 75, 7537-7541.

Shen, Y., Zhou, H., Xu, J., Wang, Y., Zhang, Q., Walsh, T.R., Shao, B., Wu, C., Hu, Y., Yang, L., Shen, Z., Wu, Z., Sun, Q., Ou, Y., Wang, Y., Wang, S., Wu, Y., Cai, C., Li, J., Shen, J., Zhang, R., Wang, Y., 2018. Anthropogenic and environmental factors associated with high incidence of mcr-1 carriage in humans across China. Nature Microbiol. 9, 1054-1062.

Stoesser, N., Mathers, A.J., Moore, C.E., Day, N.P.J., Crook, D.W., 2016. Colistin resistance gene mcr-1 and pHNSHP45 plasmid in human isolates of Escherichia coli and Klebsiella pneumoniae. The Lancet. Infect. Dis. 16, 285-286.

Sugden, R., Kelly, R., Davies, S., 2016. Combatting antimicrobial resistance globally. Nature Microbiol. 1, 16187.

Sun, M., Ye, M., Schwab, A.P., Li, X., Wan, J., Wei, Z., Wu, J., Friman, V.P., Liu, K., Tian, D., Liu, M., Li, H., Hu, F., Jiang, X., 2016. Human migration activities drive the fluctuation of ARGs: Case study of landfills in Nanjing, eastern China. J. Hazard. Mater. 315, 93-101.

Tomasz, A., 2006. Microbiology. Weapons of microbial drug resistance abound in soil flora. Science 311, 342-343.

Vaz-Moreira, I., Nunes, O.C., Manaia, C.M., 2014. Bacterial diversity and antibiotic resistance in water habitats: searching the links with the human microbiome. FEMS Microbiol Rev. 38, 761-778.

Vikesland, P.J., Pruden, A., Alvarez, P.J.J., Aga, D., Burgmann, H., Li, X.D., Manaia, C.M., Nambi, I., Wigginton, K., Zhang, T., Zhu, Y.G., 2017. Toward a Comprehensive Strategy to Mitigate Dissemination of Environmental Sources of Antibiotic Resistance. Environ. Sci. Technol. 51, 13061-13069.

Walsh, T.R., Weeks, J., Livermore, D.M., Toleman, M.A., 2011. Dissemination of NDM-1 positive bacteria in the New Delhi environment and its implications for human health: an environmental point prevalence study. The Lancet. Infect. Dis. 11, 355-362.

Wang, P., Wu, D., You, X., Su, Y., Xie, B., 2020. Antibiotic and metal resistance genes are closely linked with nitrogen-processing functions in municipal solid waste landfills. J. Hazard. Mater. 299, 215 – 221.

WHO, 2014. Antimicrobial resistance: global report on surveillance. France.

Wilson, D., Rodic, L., Modak, P., Soos, R., Carpintero, A., Velis, K., Iyer, M., Simonett, O., 2015. Global Waste Management Outlook. United Nations Environment Programme (UNEP) & International Solid Waste Association (ISWA), Nairobi.

Wu, D., Dolfing, J., Xie, B., 2018a. Bacterial perspectives on the dissemination of antibiotic resistance genes in domestic wastewater bio-treatment systems: beneficiary to victim. Applied Microbiol. Biotechnol. 102, 597-604.

Wu, D., Huang, X.H., Sun, J.Z., Graham, D.W., Xie, B., 2017. Antibiotic Resistance Genes and Associated Microbial Community Conditions in Aging Landfill Systems. Environ. Sci. Technol. 51, 12859-12867.

Wu, D., Huang, Z., Yang, K., Graham, D., Xie, B., 2015a. Relationships between antibiotics and antibiotic resistance gene levels in municipal solid waste leachates in Shanghai, China. Environ. Sci. Technol. 49, 4122-4128.

Wu, D., Ma, R., Wei, H., Yang, K., Xie, B., 2018b. Simulated discharge of treated landfill leachates reveals a fueled development of antibiotic resistance in receiving tidal river. Environ. Int. 114, 143-151.

Wu, D., Su, Y., Xi, H., Chen, X., Xie, B., 2019. Urban and agriculturally influenced water contribute differently to the spread of antibiotic resistance genes in a mega-city river network. Water Res. 158, 11-21.

Wu, D., Wang, T., Huang, X., Dolfing, J., Xie, B., 2015b. Perspective of harnessing energy from landfill leachate via microbial fuel cells: novel biofuels and electrogenic physiologies. Appl. Microbiol. Biotechnol. 99, 7827-7836.

Xie, J., Jin, L., He, T., Chen, B., Luo, X., Feng, B., Huang, W., Li, J., Fu, P., Li, X., 2019. Bacteria and Antibiotic Resistance Genes (ARGs) in PM2.5 from China: Implications for Human Exposure. Environ. Sci. Technol. 53, 963-972.

Yu, Z., He, P., Shao, L., Zhang, H., Lu, F., 2016. Co-occurrence of mobile genetic elements and antibiotic resistance genes in municipal solid waste landfill leachates: A preliminary insight into the role of landfill age. Water Res. 106, 583-592.

Zhao, R., Feng, J., Yin, X., Liu, J., Fu, W., Berendonk, T.U., Zhang, T., Li, X., Li, B., 2018. Antibiotic resistome in landfill leachate from different cities of China deciphered by metagenomic analysis. Water Res. 134, 126-139.

498 Zhu, Y.G., Zhao, Y., Li, B., Huang, C.L., Zhang, S.Y., Yu, S., Chen, Y.S., Zhang, T.,
499 Gillings, M.R., Su, J.Q., 2017. Continental-scale pollution of estuaries with antibiotic
500 resistance genes. Nat. Microbiol. 2, 16270.

Legends of Tables

Table 1 Relative abundance of integrons and physiochemical properties of landfill leachate samples

Legends of Figures

Fig. 1 Relative abundance (log_{10}(ARGs copies/16S rRNA gene copies)) of target ARGs in different landfilling periods. The bold black lines in boxplots indicated the means of log10-transferred values of detected ARGs.

Fig. 2 Distribution and relative abundance (percentages were scaled before plotting) of sequenced bacterial community at phylum and order levels. Samples were separated into 3 stages and the dominant bacteria were labeled with *** (>2.5% of total sequences). The color keys of the heatmap column represented the upper taxon-phylum of bacterial orders.

Fig. 3 Distribution of identified HBPs in landfill leachates. The red, green, and blue dots represented samples collected from Stage-1, Stage-2, and Stage-3, respectively. The distance between each sample dots was calculated based on Bray-Curtis distance (Meta-MDS). The red, green, blue regions indicated that the variations of the pathogenic bacterial community in these areas where encircled dots were samples that were majorly influenced by *Firmicutes*, *Actinobacteria*, and *Proteobacteria*,

519 respectively. The specific influential pathogens (triangle) were labeled with species
520 names.

521 **Fig**. **4** (a) The correlations between identified HBPs and target genes (red (ARGs) and
522 blue (integrons) at different landfilling periods; the coefficients from significant
523 relationships (Pearson; $P < 0.05$) were extracted to calculate the connectivity index. (b)
524 structural association between pathogenic bacteria (square) and ARGs (circle) in Stage-
525 1 (red), Stage-2 (green), and Stage-3 (grey).

526 **Fig**. **5** The distribution of identified HBPs in leachates samples from Stage-1 to Stage-
527 3. The red dots indicate bacterial pathogen species and their sizes are proportional to
528 their relative abundance in the HBPs community. The red, green, and blue areas covered
529 the Firmicutes, Actinobacteria, and *Proteobacteria* pathogens, respectively. The black,
530 yellow, and red segments connected the domain (bacteria), phyla, and classes of
531 identified pathogen species.

532 **Fig**. **6** The relative abundances of *Proteobacteria* (blue circles), *Firmicutes* (red dots),
533 and *Actinobacteria* (green squares) were linearly regressed with the activity of nitrogen
534 metabolism (Tax4Fun). The significant and insignificant regressions were depicted in
535 sold and dash lines, respectively. The shades indicated the confidential intervals of
536 significant correlations (IC= 95%)

*Declaration of Interest Statement

Declaration of interests

☒ The authors declare that they have no known competing financial interests or personal relationships that could have appeared to influence the work reported in this paper.

☐The authors declare the following financial interests/personal relationships which may be considered as potential competing interests:

CRediT author statement

Dong Wu: Conceptualization, Methodology, Software, Data Curation, Visualization, Writing - Original Draft; **Liuhong Wang**: Conceptualization, Methodology, Data curation; **Yinglong Su**: Visualization, Investigation, Project administration; **Jan Dolfing**: Writing- Reviewing and Editing, Data curation; **Bing Xie**: Conceptualization, Project administration, Funding acquisition, Writing, Supervision.

Table 1 Relative abundance of integrons and physiochemical properties of landfill leachate samples

Samples (n = 12)	[a] *intl1/2* log_{10}(copies/16S)	pH	DO (mg/L)	NH_4^+-N (mg/L)	[b] NO_2^-/NO_3^--N (mg/L)	TN (mg/L)	TP (mg/L)	COD (mg/L)
[c] Stage-1	-1.5±0.2 -2.8±0.5	7.4±0.4	1.0±0.4	777.2±281.2	20.7±17.6	3554.0±290.6	6.9±2.5	484.8±203.1
Stage-2	-1.4±0.2 -3.4±0.4	7.7±0.5	0.9±0.6	227.1±156.4	5.7±4.2	1321.4±195.2	2.8±1.4	572.3±141.0
Stage-3	-1.3±0.2 -2.9±0.5	7.6±0.7	1.4±0.3	173.9±73.1	11.6±6.3	599.1±37.4	0.4±0.4	292.6±154.2

[a] The abundances of intl1 and intl2 were listed in upper and lower rows, respectively

[b] Total concentrations of nitrate-N and nitrite-N (nitrite accounted for < 5% of the summed values)

[c] Leachate samples were collected 60 days after the commencement of the landfill experiment.

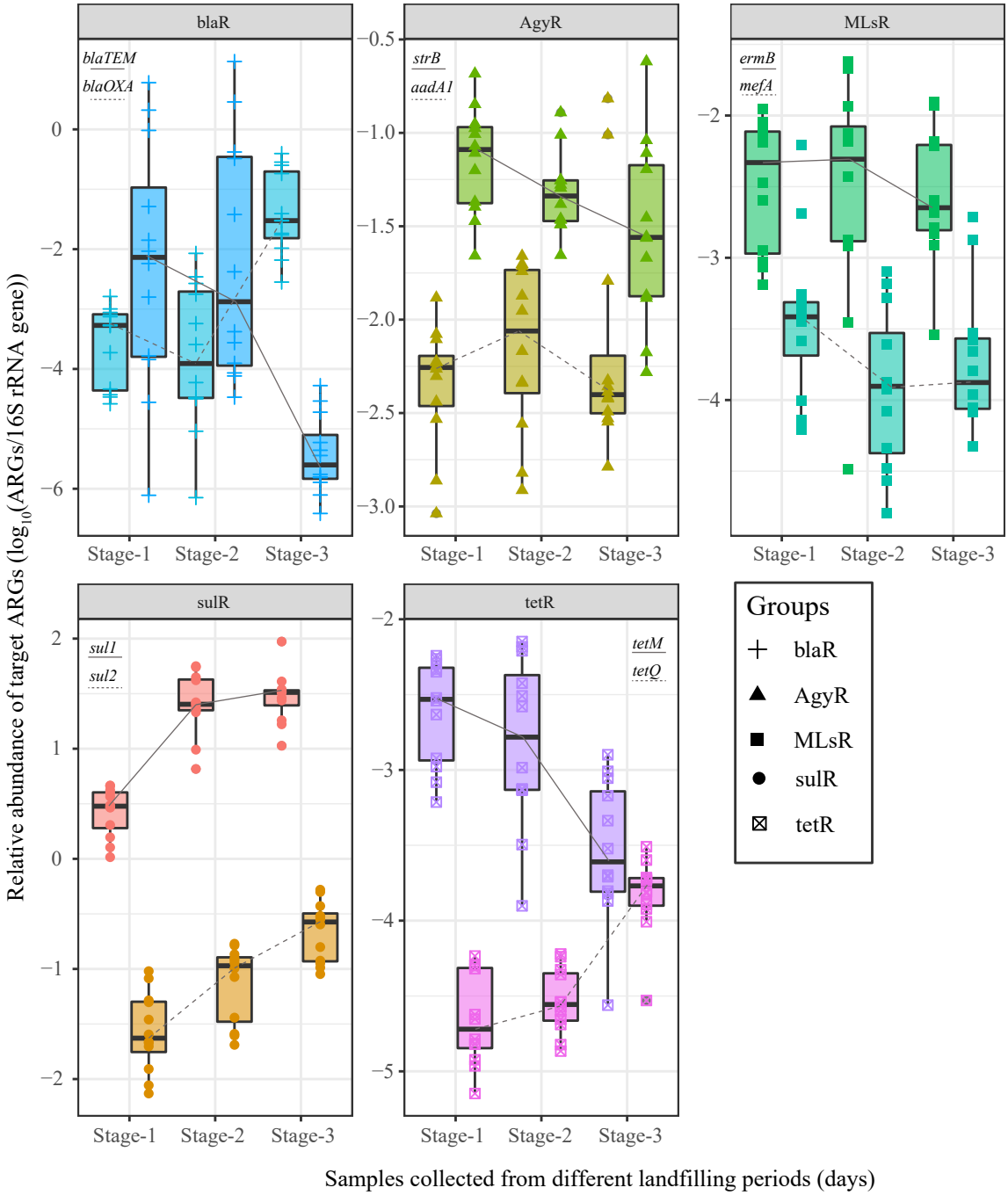

Fig. 1 Relative abundance (log_{10}(ARGs copies/16S rRNA gene copies)) of target ARGs in different landfilling periods. The bold black lines in boxplots indicated the means of log_{10}-transferred values of detected ARGs..

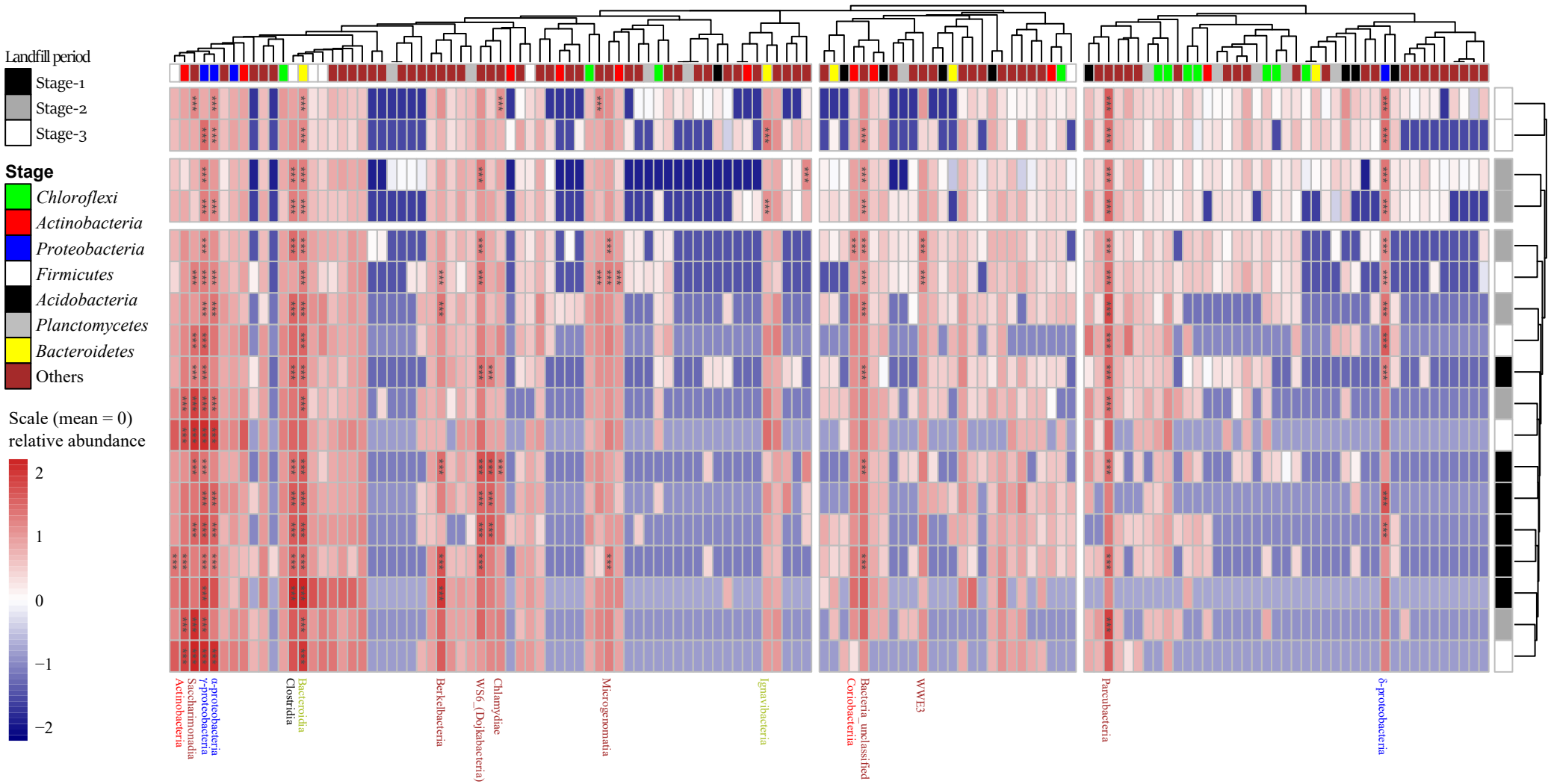

Fig.2 Distribution and relative abundance (percentages were scaled before plotting) of sequenced bacterial community at phylum and order levels. Samples were separated into 3 stages and the dominant bacteria were labelled with "***" (>2.5% of total sequences). The color keys of the heatmap column represented the upper taxon-phylum of bacterial orders.

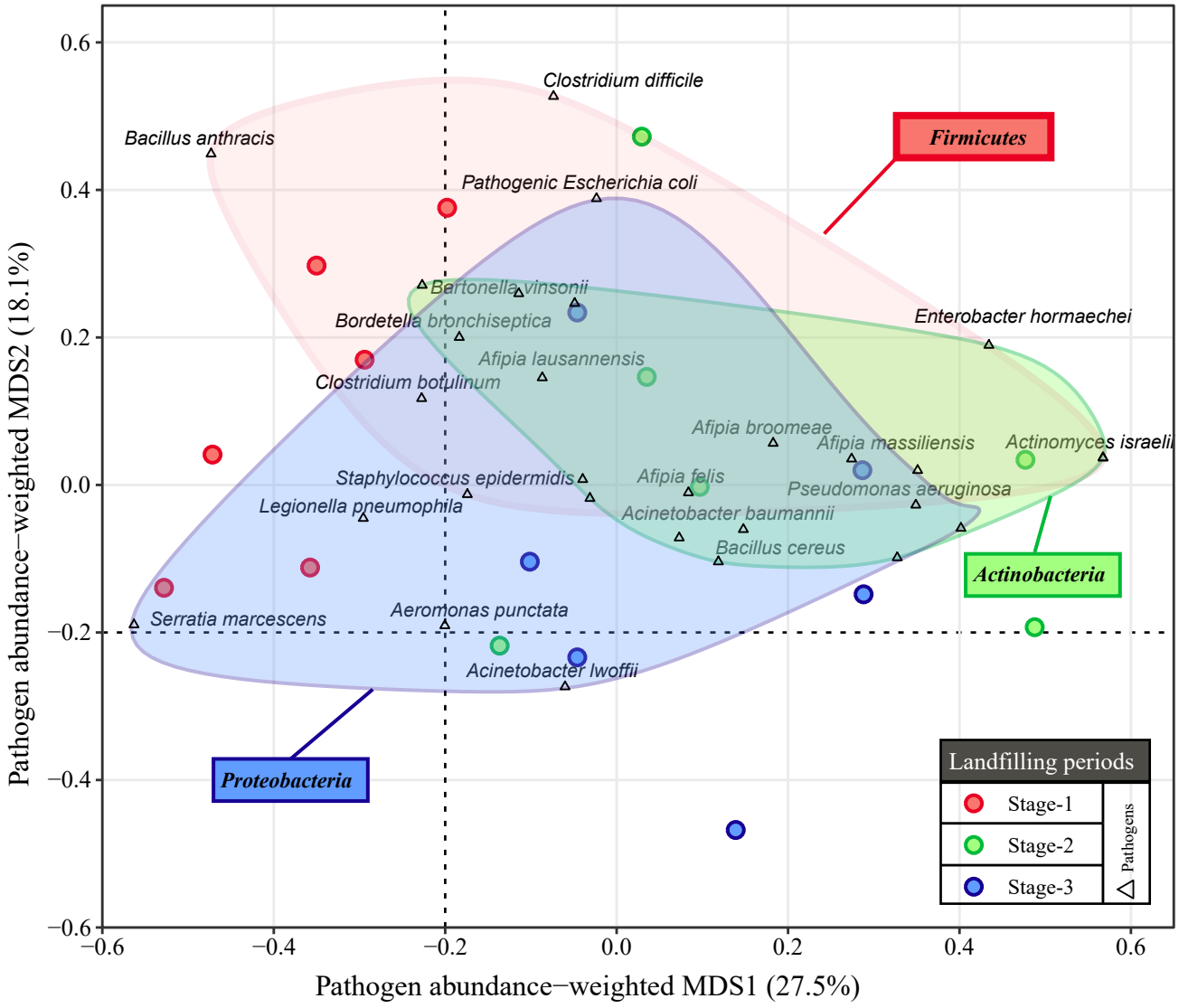

Fig.3 Distribution of identified HBPs in landfill leachates. The red, green, and blue dots represented samples collected from Stage-1, Stage-2, and Stage-3, respectively. The distance between each sample dots was calculated based on Bray-Curtis distance (Meta-MDS). The red, green, blue regions indicated that the variations of the pathogenic bacterial community in these areas where encircled dots were samples that were majorly influenced by *Firmicutes*, *Actinobacteria*, and *Proteobacteria*, respectively. The specific influential pathogens (triangle) were labeled with species names.

Figure 4

Click here to access/download;Figure;Figure 4.pdf

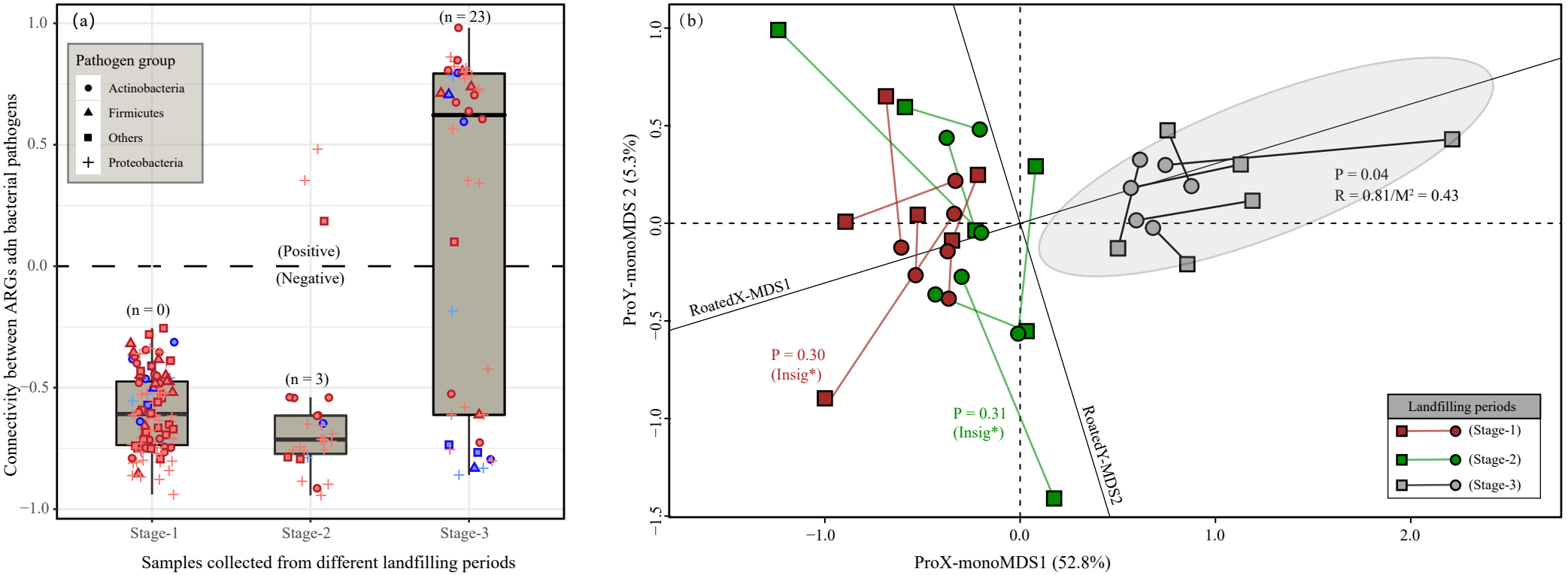

Fig. 4 (**a**) The correlations between identified HBPs and target genes (red (ARGs) and blue (integrons) at different landfilling periods; the coefficients from significant relationships (Pearson; $P < 0.05$) were extracted to calculate the connectivity index. (**b**) structural association between pathogenic bacteria (square) and ARGs (circle) in Stage-1 (red), Stage-2 (green), and Stage-3 (grey).

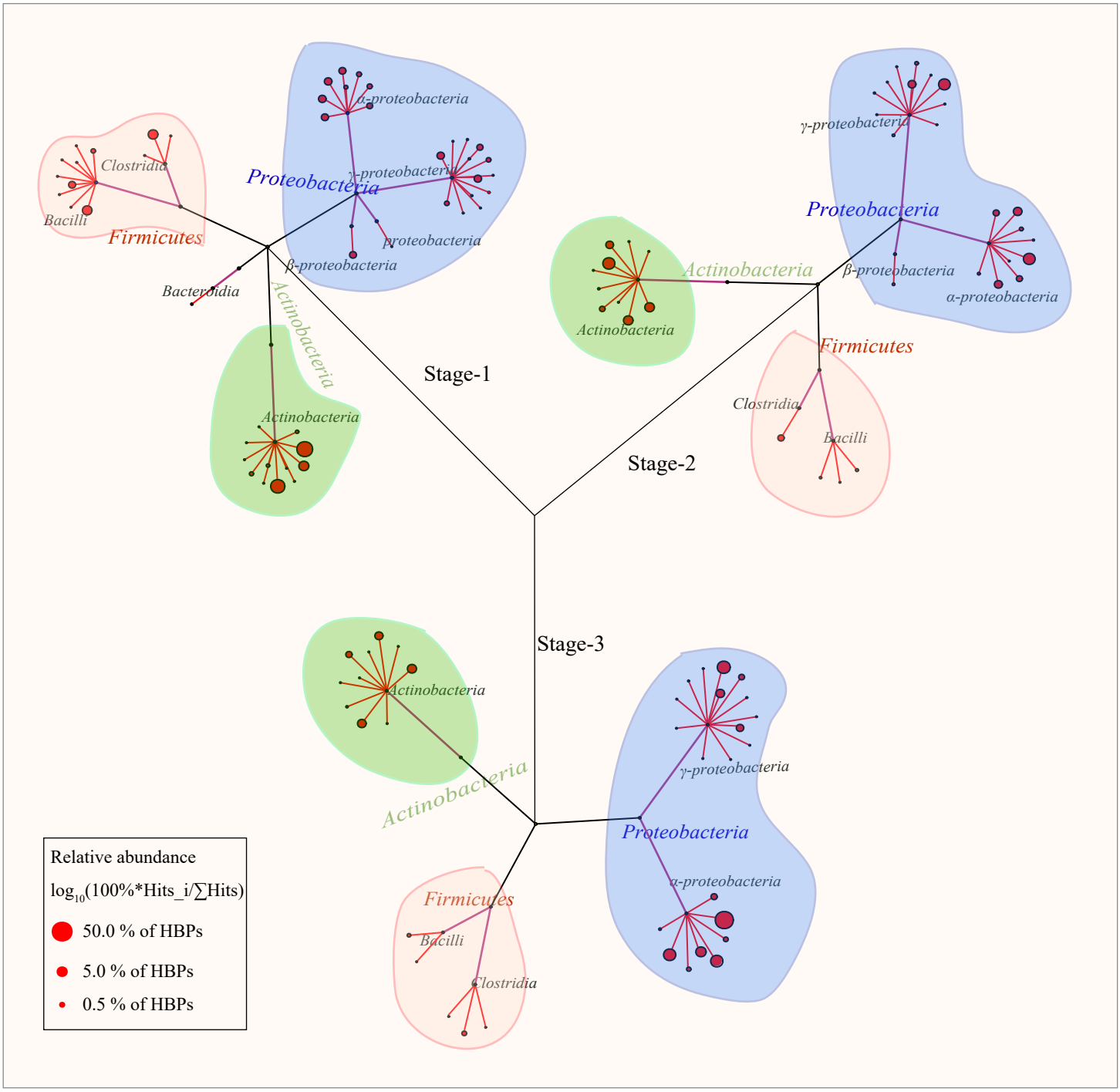

Fig. 5 The distribution of identified HBPs in leachates samples from Stage-1 to Stage-3. The red dots indicate bacterial pathogen species and their sizes are proportional to their relative abundance in the HBPs community. The red, green, and blue areas covered the *Firmicutes*, *Actinobacteria*, and *Proteobacteria* pathogens, respectively. The black, yellow, and red segments connected the domain (bacteria), phyla, and classes of identified pathogen species.

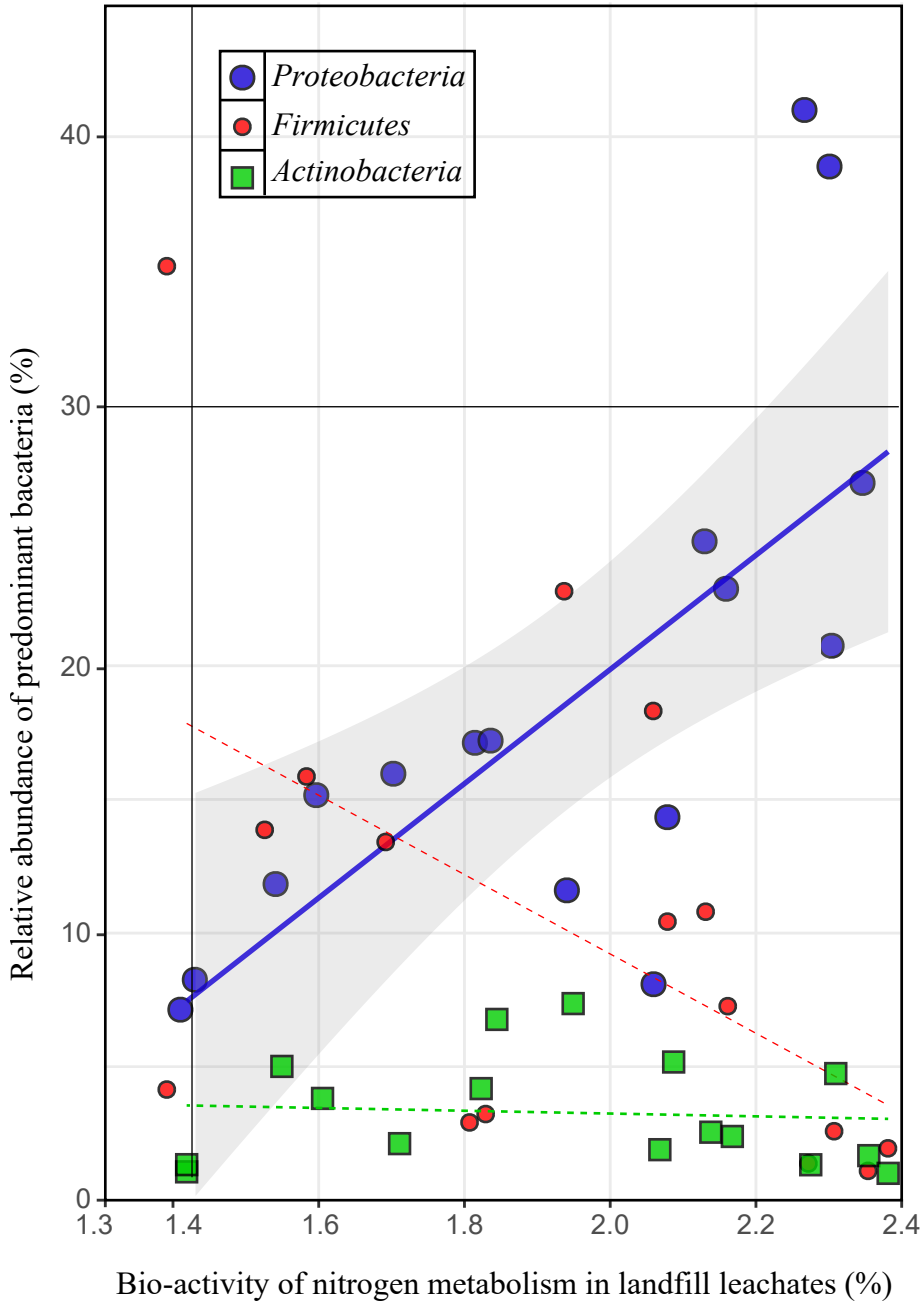

Fig. 6 The relative abundances of *Proteobacteria* (blue circles), *Firmicutes* (red dots), and *Actinobacteria* (green squares) were linearly regressed with the activity of nitrogen metabolism (Tax4Fun). The significant and insignificant regressions were depicted in sold and dash lines, respectively. The shades indicated the confidential intervals of significant correlations (IC= 95%)